

Single Phase Lock Loop

davide bagnara

December 3, 2025

Contents

1	Introduction	3
2	Nomenclature	3
3	Basic Structure of a Phase-Locked Loop	4
4	SOGI-QSG-based PLL	5

List of Figures

1	Basic structure of a PLL.	4
2	Block diagram of an elementary <i>PLL</i>	4
3	Small signal model of an elementary <i>PLL</i>	5
4	Voltage controlled oscillator based on a adaptive filter.	6
5	Quadrature signal generator based on a adaptive filter.	7
6	Second order adaptive filter based on an second order generalized integrator and a quadrature signal generator (<i>SOGI-QSG</i>).	8
7	Diagram of the <i>SOGI</i> -based <i>PLL</i> (<i>SOGI-QSG</i>).	8
8	Bode diagram of the <i>SOGI-QSG</i> response.	9
9	PLL based on the on direct and inverse Park transform.	9
10	Equivalent block diagram of the PLL based on the on direct and inverse Park transform.	9
11	Bode diagram of the <i>QSG-PLL</i> based on direct and inverse Parck transform.	10

List of Tables

1 Introduction

In this document the following topics are slightly covered:

- phase locked loop for single phase signals;
- moving average filter;
- discrete Fourier transform;
- Simulink C-caller;
- dSPACE SCALEXIO.

The idea of the document is to propose an laboratory application of a single-phase *PLL*, and moving average filter implemented in a fast prototyping equipment. The moving average filter will be implemented using customized C-code and Simulink C-caller.

2 Nomenclature

Here a list of symbols, variables, and parameters used along the document:

- *PLL*: phase locked loop;
- *VCO*: voltage controlled oscillator;
- *PI*: proportional integral controller;
- *LF*: loop filter;
- *PD*: phase detector;
- *SOGI*: second order generalized integrator;
- *QSG*: quadrature signal generator;
- *MAVG*: moving average;
- RMB: right mouse button;
- LMB: left mouse button;
- HMI: human machine interface;
- ConfigurationDesk: dSPACE application used to configure a project with the scalexio equipment;
- ControlDesk: dSPACE application used as HMI;
- $v, v_{signal} \left[V \right]$: input signals;
- $\alpha\beta$: direct and quadrature components of a vector quantity, generally with respect to a stationary reference frame;
- $\xi\eta$: additional direct and quadrature components of a vector quantity, generally with respect to a rotating reference frame;

3 Basic Structure of a Phase-Locked Loop

The basic structure of the phase-locked loop (*PLL*) is shown in Figure 1. It consists of three fundamental blocks:

- *phase detector (PD)*. This block generates an output signal proportional to the phase difference between the input signal, v_{signal} , and the signal generated by the internal oscillator of the *PLL*, v^{pll} . Depending on the type of *PD*, high frequency AC components appear together with the DC phase-angle difference signal.
- *loop filter (LF)*. This block presents a low pass filtering characteristic to attenuate the high frequency AC components from the *PD* output. Typically, this block is constituted by a first order low pass filter or a PI controller.
- *voltage controlled oscillator (VCO)*. This block generates at its output an AC signal whose frequency is shifted with respect to a given central frequency, ω_{ff} , as a function of the input voltage provided by the *LF*.

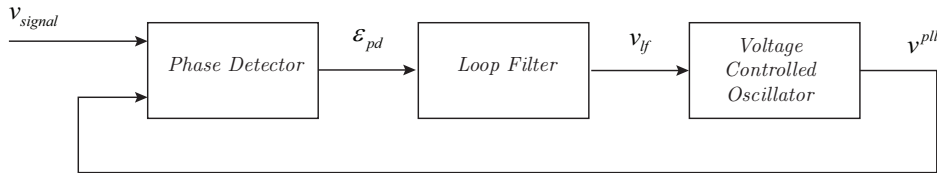


Figure 1: Basic structure of a PLL.

The block diagram of an elementary *PLL* is shown in Figure 2. In this case *PD* is implemented by means of the *Superheterodyne* technique, the *LF* is based on a *PI* controller and the *VCO* consists of a sinusoidal function supplied by a linear integrator.

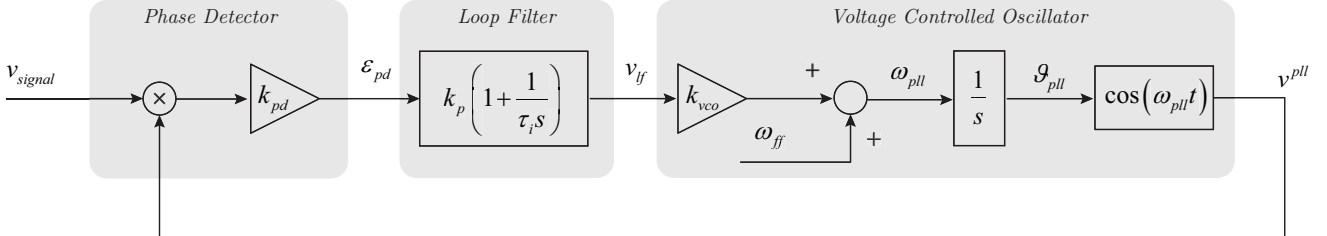


Figure 2: Block diagram of an elementary *PLL*.

If the input signal applied to this system is given by

$$v = V \sin(\vartheta) = V \sin(\omega t + \phi) \quad (3.1)$$

and the signal generated by the *VCO* is given by

$$v^{pll} = \cos(\vartheta_{pll}) = \cos(\omega_{pll}t + \phi_{pll}) \quad (3.2)$$

the phase error signal from the multiplier *PD* output can be written as

$$\begin{aligned} \varepsilon_{pd} &= V k_{pd} \sin(\omega t + \phi) \cos(\omega_{pll}t + \phi_{pll}) \\ &= \frac{V k_{pd}}{2} \left[\sin[(\omega - \omega_{pll})t + (\phi - \phi_{pll})] + \sin[(\omega + \omega_{pll})t + (\phi + \phi_{pll})] \right] \end{aligned} \quad (3.3)$$

The high frequency components ($\omega + \omega_{pll}$) of the *PD* error signal will be cancelled out by the *LF*, only the low frequency term ($\omega - \omega_{pll}$) will be processed, therefore, the *PD* error signal to be considered is

$$\varepsilon_{pd} = \frac{V k_{pd}}{2} \sin[(\omega - \omega_{pll})t + (\phi - \phi_{pll})] \quad (3.4)$$

If it is assumed that the *VCO* is well tuned to the input frequency, i.e. with $\omega \approx \omega_{pll}$, the DC term of the phase error is given as follows

$$\varepsilon_{pd} = \frac{V k_{pd}}{2} \sin(\phi - \phi_{pll}) \quad (3.5)$$

It can be observed in (3.5) that the multiplier *PD* produces nonlinear phase detection because of the sinusoidal function. However, when phase error is very small, i.e. when $\phi \approx \phi_{pll}$, the output of the multiplier *PD* can be linearized in the vicinity of such an operating point since $\sin(\phi - \phi_{pll}) \approx \sin(\vartheta - \vartheta_{pll}) \approx (\vartheta - \vartheta_{pll})$. Therefore, once the *PLL* is locked, the relevant term of the phase error signal is given by

$$\varepsilon_{pd} = \frac{V k_{pd}}{2} (\vartheta - \vartheta_{pll}) \quad (3.6)$$

According to Eq. (3.6), the model presented in Figure 2 can be linearized around the condition of $\omega \approx \omega_{pll}$ resulting as per Figure 3.

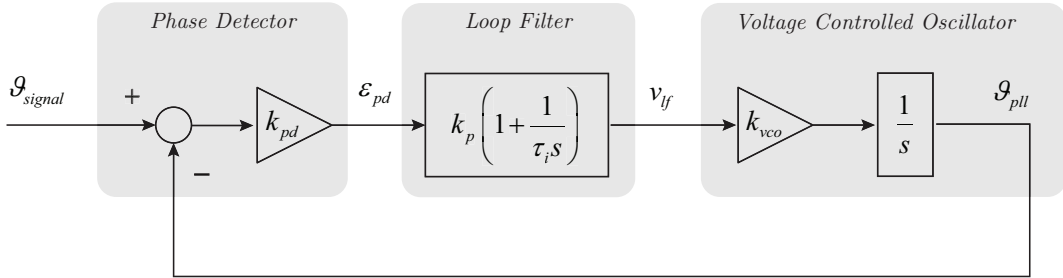


Figure 3: Small signal model of an elementary *PLL*.

According to the block diagram of Figure 3 a frequency domain analysis brings to the following transfer functions (consider $k_{pd} = k_{vco} = 1$):

$$H(s) = PD(s)LF(s)VCO(s) = \frac{k_p s + \frac{k_p}{\tau_i}}{s^2} \quad (3.7)$$

$$H_\vartheta(s) = \frac{\Theta_{pll}(s)}{\Theta(s)} = \frac{H(s)}{1 + H(s)} = \frac{k_p s + \frac{k_p}{\tau_i}}{s^2 + k_p s + \frac{k_p}{\tau_i}} \quad (3.8)$$

$$E_\vartheta = \frac{E_{pd}(s)}{\Theta(s)} = 1 - H_\vartheta(s) = \frac{s^2}{s^2 + k_p s + \frac{k_p}{\tau_i}} \quad (3.9)$$

The open loop transfer function of Eq. (3.7) shows that the *PLL* has two poles at the origin, which means that is able to track even a constant slope ramp in the input phase angle without any steady state error.

4 SOGI-QSG-based PLL

Figure 4 shows the structure of a *VCO* based on *QSG*; the structure consists of an adaptive filter.

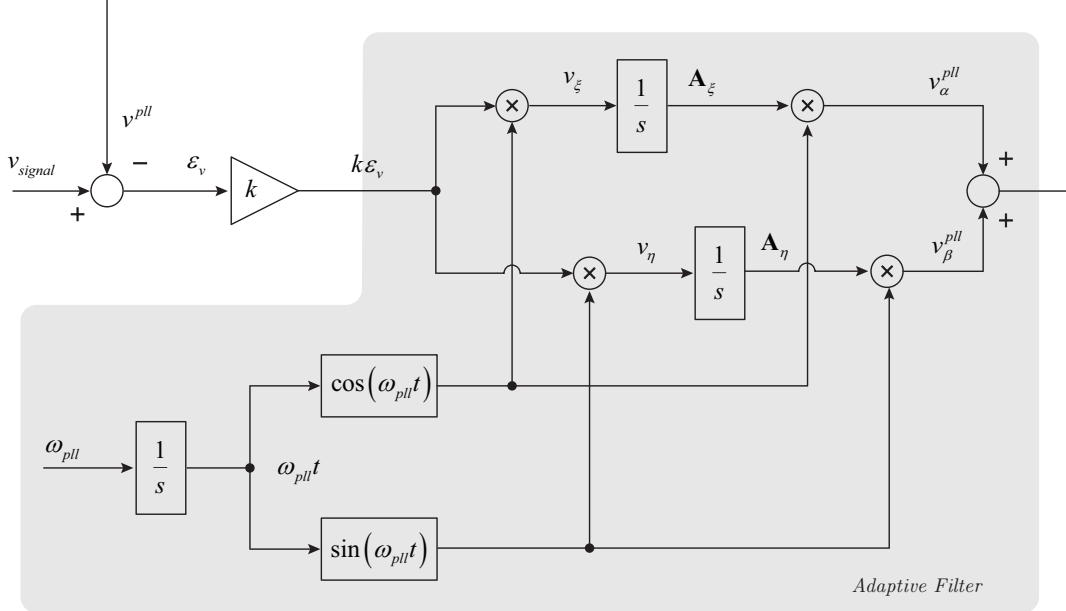


Figure 4: Voltage controlled oscillator based on a adaptive filter.

Defining $g = k\epsilon_v$, the v_ξ , and v_η components of Figure 4 can be written as follows

$$v_\xi = g \cos(\omega_{pll}) = \frac{1}{2}g(e^{j\omega_{pll}t} + e^{-j\omega_{pll}t}) \quad (4.1)$$

$$v_\eta = g \cos(\omega_{pll}) = -j\frac{1}{2}g(e^{j\omega_{pll}t} - e^{-j\omega_{pll}t}) \quad (4.2)$$

The \mathbf{A}_ξ , and \mathbf{A}_η terms which correspond to the output of the integrators for v_ξ and v_η , can be expressed in the Laplace domain as follows

$$\mathbf{A}_\xi = \frac{1}{s}v_\xi(s) = \frac{1}{2s}\left[g(s + j\omega_{pll}t) + g(s - j\omega_{pll}t)\right] \quad (4.3)$$

$$\mathbf{A}_\eta = \frac{1}{s}v_\eta(s) = -j\frac{1}{2s}\left[g(s + j\omega_{pll}t) - g(s - j\omega_{pll}t)\right] \quad (4.4)$$

and the v_α^{pll} , v_β^{pll} terms result as follows

$$\begin{aligned} v_\alpha^{pll} &= \frac{1}{2}\left[\mathbf{A}_\xi(s + j\omega_{pll}t) + \mathbf{A}_\xi(s - j\omega_{pll}t)\right] \\ &= \frac{1}{4(s + j\omega_{pll})}\left[g(s) + g(s + j\omega_{pll}t)\right] + \frac{1}{4(s - j\omega_{pll})}\left[g(s) + g(s - j\omega_{pll}t)\right] \end{aligned} \quad (4.5)$$

$$\begin{aligned} v_\beta^{pll} &= -j\frac{1}{2}\left[\mathbf{A}_\xi(s + j\omega_{pll}t) - \mathbf{A}_\xi(s - j\omega_{pll}t)\right] \\ &= \frac{1}{4(s + j\omega_{pll})}\left[g(s) + g(s + 2j\omega_{pll}t)\right] + \frac{1}{4(s - j\omega_{pll})}\left[g(s) - g(s - 2j\omega_{pll}t)\right] \end{aligned} \quad (4.6)$$

The term $v^{pll} = v_\alpha^{pll} + v_\beta^{pll}$ results as follows

$$v^{pll} = v_\alpha^{pll} + v_\beta^{pll} = \frac{s}{s^2 + \omega_{pll}^2}g(s) \quad (4.7)$$

Consequently, the transfer functions of the adaptive filter VCO structure of Figure 4 are given by

$$\frac{v^{pll}}{\varepsilon_v}(s) = \frac{ks}{s^2 + \omega_{pll}^2} \quad (4.8)$$

$$\frac{v^{pll}}{v}(s) = \frac{ks}{s^2 + ks + \omega_{pll}^2} \quad (4.9)$$

$$\frac{\varepsilon_v}{v}(s) = \frac{s^2 + \omega_{pll}^2}{s^2 + ks + \omega_{pll}^2} \quad (4.10)$$

The structure of Figure 4 can be used of quadrature signal generator (*QSG*) by adding a scaled integrator at the output of the adaptive filter, as in Figure 5 is shown.

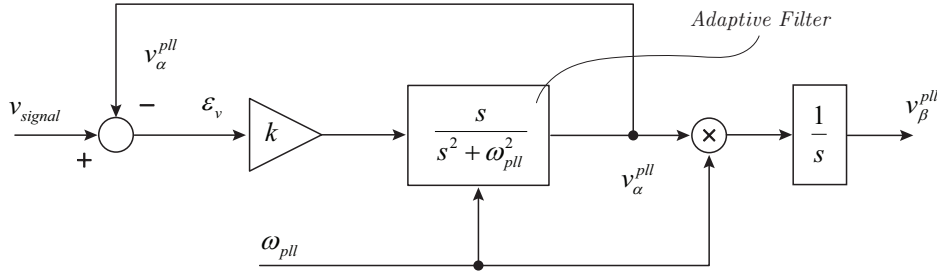


Figure 5: Quadrature signal generator based on a adaptive filter.

Clearly, the response of the AF block, shown in Figure 4 is defined by Eq. (4.8) in the case of applying a likewise sinusoidal signal (sine or cosine) with frequency ω_{pll} to its input.

Recalling that

$$\mathcal{L}[\sin(\omega_{pll})] = \frac{\omega_{pll}}{s^2 + \omega_{pll}^2} \quad (4.11)$$

$$\mathcal{L}[\cos(\omega_{pll})] = \frac{s}{s^2 + \omega_{pll}^2} \quad (4.12)$$

the time response of the system characterized by Eq. (4.8) in the presence of sinusoidal inputs is given by

$$\mathcal{L}^{-1}\left[\frac{\omega_{pll}}{s^2 + \omega_{pll}^2} \frac{s}{s^2 + \omega_{pll}^2}\right] = \frac{1}{2}t \sin(\omega_{pll}t) \quad (4.13)$$

and

$$\mathcal{L}^{-1}\left[\frac{s}{s^2 + \omega_{pll}^2} \frac{s}{s^2 + \omega_{pll}^2}\right] = \frac{1}{2} \left[\frac{\sin(\omega_{pll}t)}{\omega_{pll}} + t \cos(\omega_{pll}t) \right] \approx \frac{1}{2}t \cos(\omega_{pll}t) \quad (4.14)$$

An efficient implementation of the structure of Figure 5 is shown in Figure 6, where

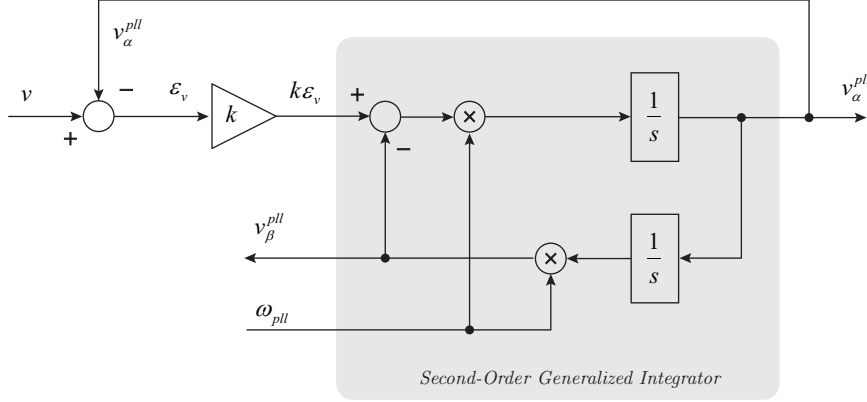


Figure 6: Second order adaptive filter based on an second order generalized integrator and a quadrature signal generator (SOGI-QSG).

$$SOGI(s) = \frac{v_{\alpha}^{pll}}{\varepsilon_v}(s) = \frac{k \omega_{pll} s}{s^2 + \omega_{pll}^2} \quad (4.15)$$

$$D(s) = \frac{v_{\alpha}^{pll}}{v}(s) = \frac{k \omega_{pll} s}{s^2 + k \omega_{pll} s + \omega_{pll}^2} \quad (4.16)$$

$$Q(s) = \frac{v_{\beta}^{pll}}{v}(s) = \frac{k \omega_{pll}^2}{s^2 + k \omega_{pll} s + \omega_{pll}^2} \quad (4.17)$$

Based on the structure of the *SOGI-QSG* of Figure 6 it is possible to implement a *SOGI-QSG*-based *PLL* as shown in Figure 7.

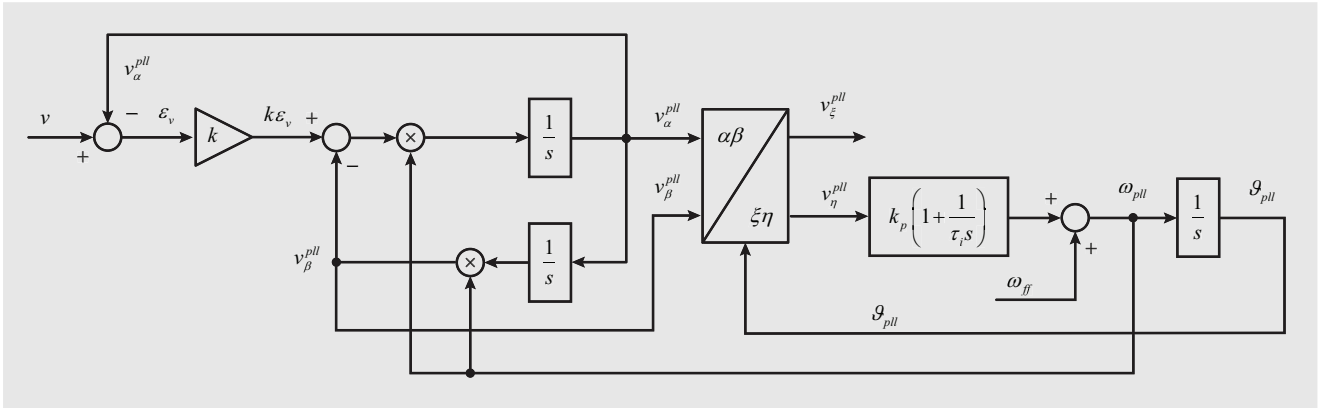
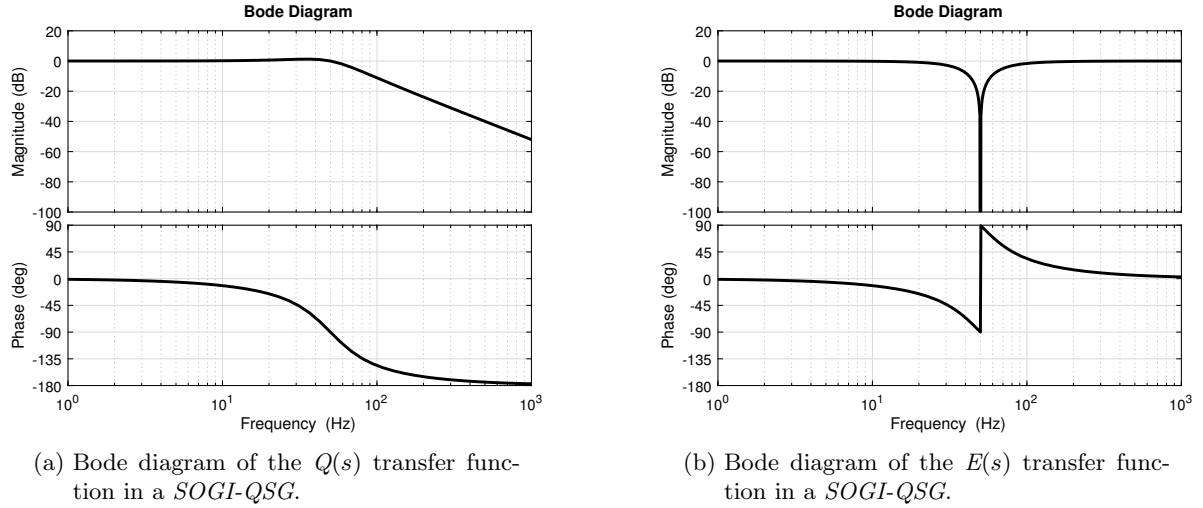


Figure 7: Diagram of the SOGI-based PLL (SOGI-QSG).

The transfer function from the input signal v to the error signal ε_v is given by

$$E(s) = \frac{\varepsilon_v}{v}(s) = \frac{s^2 + \omega_{pll}^2}{s^2 + k \omega_{pll} s + \omega_{pll}^2} \quad (4.18)$$

The transfer function of Eq. (4.18) responds to a second order notch filter, with zero gain at the centre frequency (ω_{pll}).


 Figure 8: Bode diagram of the *SOGI-QSG* response.

Another useful possible implementation of the *SOGI-QSG-based PLL* is based on the direct and inverse Park transforms, as shown in Figure 9

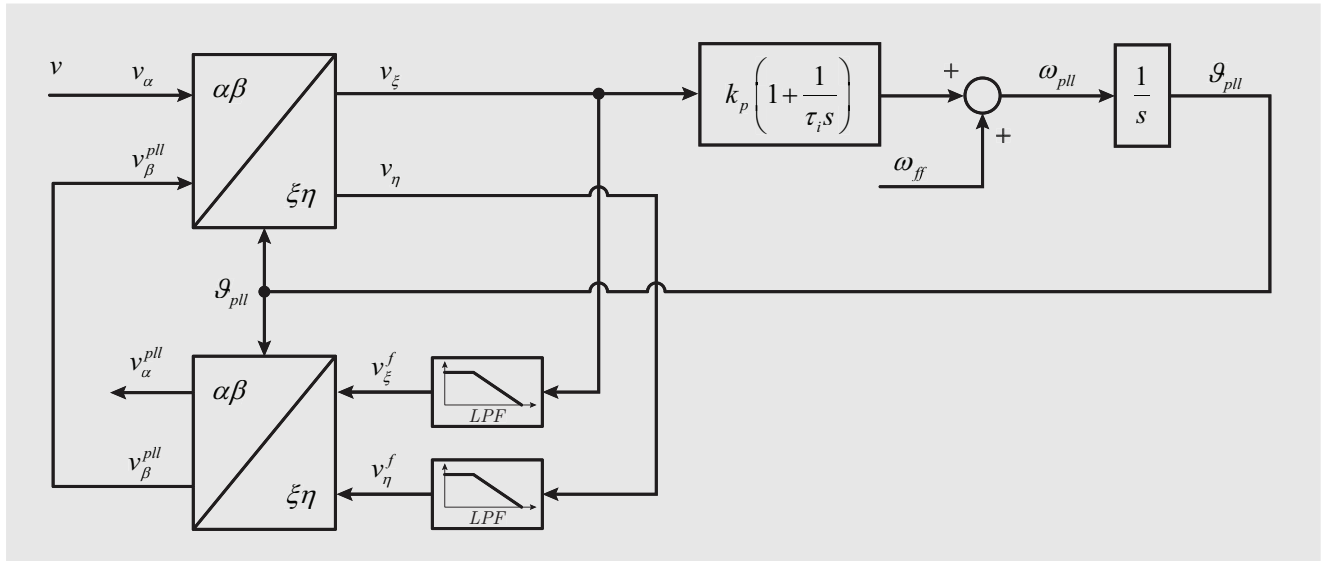


Figure 9: PLL based on the on direct and inverse Park transform.

An equivalent transfer function block diagram is presented in Figure 10. In this configuration the transformation $v_\alpha \rightarrow v_\beta^{pll}$ is represented as ω_{pll}/s in Laplace domain. An intuitive explanation of its operation principle can be given if it is assumed that the *PLL* is well tuned to the input signal frequency. Under such operation conditions, if v_α and v_β^{pll} are not in quadrature, the virtual input vector, v_α^{pll} , resulting from these signals will have neither constant amplitude nor rotation speed.

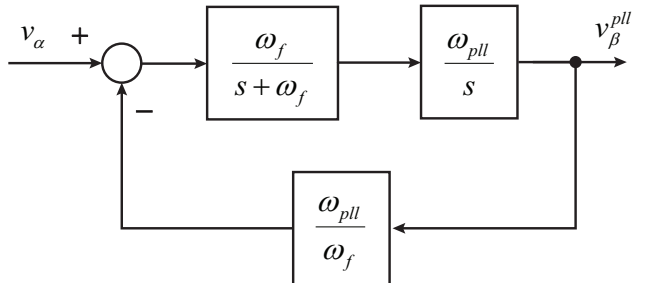


Figure 10: Equivalent block diagram of the PLL based on the on direct and inverse Park transform.

References

Therefore v_ξ and v_η waveform resulting from direct Park transformation will have harmonics components. These harmonics will be suppressed by the *LPF* blocks generating, as well, the components v_ξ^f and v_η^f . The v_α and v_β^{pll} components resulting from the inverse Park transformation of

the components v_ξ^f and v_η^f will be in quadrature, though v_α and v_α^{pll} will not be in phase if the *PLL* is not perfectly synchronized. As the *PLL* locks the phase angle of the input signal v_α , the components v_α^{pll} and v_β^{pll} will be respectively in phase and in quadrature respect to the input signal v_α .

From the equivalent block diagram of Figure 10 the following transfer functions can be derived

$$\boxed{\frac{V_\beta^{pll}}{V_\alpha}(s) = \frac{\omega_f \omega_{pll}}{s^2 + \omega_f s + \omega_{pll}^2}} \quad (4.19)$$

$$\boxed{\frac{V_\alpha^{pll}}{V_\alpha}(s) = \frac{s \omega_f}{s^2 + \omega_f s + \omega_{pll}^2}} \quad (4.20)$$

where the relation of Eq. (4.21) has been applied.

$$V_\beta^{pll}(s) = \frac{\omega_{pll}}{s} V_\alpha^{pll}(s) \quad (4.21)$$

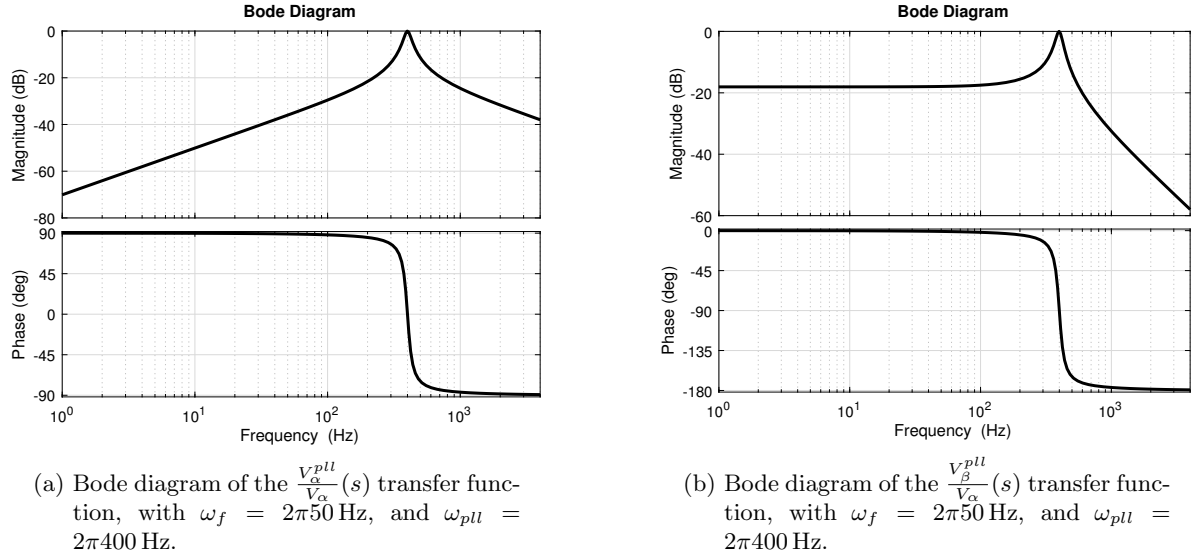


Figure 11: Bode diagram of the *QSG-PLL* based on direct and inverse Park transform.

References

- [1] R. Teodorescu, M. Liserre, P. Rodriguez, *Grid converters for photovoltaic and wind power systems*. Wiley, 2011.